Lee et al. EURASIP Journal on Wireless Communications and Networking (2017) 2017:142
DOI 10.1186/s13638-017-0928-x

EURASIP Journal on Wireless Communications and Networking

RESEARCH Open Access

# A spatial slotted-Aloha protocol in wireless networks for group communications

Mingyu Lee, Yunmin Kim and Tae-Jin Lee*

**Abstract**

In a large-scale group communication networks, we propose a slotted-Aloha-based access control (SA-AC) scheme with the optimal transmission probability (TP) using the stochastic geometry. Since the performance of SA-AC scheme depends on the TP of the members in a group, the analytical model presents a joint view for the downlink (DL) and the uplink (UL) with TP of the members in a group. We present simple and closed form expressions for the DL and UL joint probability by using Poisson point process (PPP). Furthermore, we analyze the dynamic TP and the optimal TP to maximize the DL/UL joint probability, for which the inclusion of a member and the transmission of the member is determined by the DL and UL thresholds. Since the requirement of the DL/UL joint probability varies with the type of services, the optimal TP has to be determined for an efficient group communication service. The performance of the SA-AC scheme with the optimal TP is demonstrated, and it is shown to be superior over the other schemes.

**Keywords:** Group communication, Spatial Aloha, Stochastic geometry

## 1 Introduction

In a large-scale group communication network, some nodes may form a cluster and clusters communicate with one another. For example, in a tactical group communication network, a commander monitors the conditions of the soldiers. A soldier equips with a monitoring system [1], and the monitored status is transmitted to the base camp through an unmanned aerial vehicle (UAV) [2]. If all the soldiers transmit their information at the same time to the UAV, the network congestion will occur increasingly as the number of soldiers increases. Thus, a hierarchical system in which relays or vehicles collect the information of the soldiers and they transmit the collected information to the UAV could be desirable. In the system, the soldiers are grouped to communicate with a relay or a vehicle, and they act as the group members and the relay or the vehicle becomes the group leader. The group leader has to cover the group members as many as possible within its communication range. The members have to choose the best group leader among the candidate group leaders. The group leader will control the transmissions of the group members within its coverage.

*Correspondence: tjlee@skku.edu
College of Information and Communication Engineering, Sungkyunkwan University, Suwon 16419, South Korea

With a massive number of nodes, the group leaders and the members form a large-scale network and they can be modeled by the Poisson point process (PPP). PPP is a spatial point process, which is widely used to model a wireless network. However, a large-scale network with group communications in which group leaders and members send and receive information has not been studied. Since the members within the coverage of a leader are able to transmit for communications, the locations of the members are no longer independent to the location of the leader. Moreover, the interference model should be different from that in [3] because the interference from the covered area of a leader is important compared to that from the non-covered area of a leader. In addition, the covered members of a group may decide whether to transmit or not by a transmission control (TC) value, which is globally determined by the leaders in a centralized manner. Thus, a new network model to capture the behavior of hierarchical group communications needs to be setup.

Since wireless resources in a group communication network are shared in a distributed manner, the performance depends on the medium access control (MAC) scheme. In this sense, transmission probability (TP), which is decided by the TC value, should be carefully chosen. Since the TP of nodes in an Aloha-based scheme may be adaptively determined by channel variation, local topology, and target utility, a new MAC protocol can be designed by using the optimal TP which is derived from the PPP models in group communication networks.

In this paper, we first derive the dynamic TP which is determined by the statistical distributions of group leaders and the DL coverage probability. We focus on the special case to derive the closed-form expressions. The coverage probability and the average numbers of members per leader in the DL are derived for the dynamic TP. The dynamic TP has been known to be optimal in terms of the MAC layer. However, the performance using the dynamic TP has not been evaluated by considering geometrical distributions of network elements.

Next, we propose the optimal TP which maximizes the downlink (DL) and uplink (UL) joint probability. The DL/UL joint probability is that the transmission of the leader and the transmission of a member are performed within the DL coverage threshold and the UL transmission threshold. The probability is determined by the probability density function (pdf) of the distance between the leader and a member which is within the coverage of the leader. The pdf is derived and is utilized to model the UL probability and the DL/UL joint probability. Since the DL/UL joint probability is maximized for a certain distance between the leader and a member, the closed-form expressions of the optimal TP for the distance can be derived. In a practical system, the distance is usually hard to be determined. In our proposed scheme, however, a leader can determine the optimal TP by using the average number of members per leader.

Finally, we present the performance of the DL/UL joint probability and the average achievable rate for a target distance in our model. In addition, the average achievable rates for the different TPs are provided. From the analytical model, the effect of TP in a group communication network is provided. Furthermore, a new policy to determine the optimal TP is proposed by considering the geometrical effects of network elements. For the group communication network, the performance at a target distance is maximized by the proposed slotted-Aloha-based access control (SA-AC) scheme.

The contributions of our work are summarized in the following points:

- We propose a new SA-AC scheme with the optimal TP to maximize the DL/UL joint probability for group communication network.
- We define pdf of the distance between a leader and its covered member for a given DL threshold, and the closed form expression of the optimal TP to maximize the DL/UL joint probability for a target member.
- We evaluate the performance of the proposed SA-AC scheme with the traditional schemes.

The rest of this paper is organized as follows. Section 2 reviews the recent PPP studies of DL, UL, and the MAC perspectives. In Section 3, we explain the proposed SA-AC scheme and the other SA-AC schemes in group communication networks. Section 4 analyzes the dynamic TP and the optimal TP by using the PPP model and presents an access scheme with the optimal TP. Section 5 presents numerical results to demonstrate the access control schemes with different TPs. Finally, we conclude in Section 6.

## 2 Related works

Modeling of the DL of a large-scale network using stochastic geometry has been studied in [4, 5]. The performance of the DL system depends on the locations of base stations (BSs), and it has been derived by modeling BSs as a PPP [6–9]. The general expressions for the coverage probability and achievable rate at a typical user are presented in [4]. In some special cases, the closed-form expressions, which give an intuitive view for the DL system, are provided. In [5], the association probability for a certain type of BSs which are modeled as multiple PPPs with different spatial densities and system parameters is studied. The analytical model in [5] presents the outage and spectral efficiency performance for the DL system deploying different types of BSs. Most PPP models for the DL system are analyzed from the view point of a typical user with a DL communication threshold, which shows that the tractable models are fairly accurate compared to actual systems. The performance of the resource management schemes in the DL (e.g., coverage expansion [5], fractional frequency reuse (FFR) [10], and resource partitioning [11]) is analyzed by using the PPP.

The analytical model using PPP for the UL of a large-scale network has also been developed. The models in [12–14] are developed by dividing Voronoi cells from the perspective of users which are modeled as a PPP. Each user has its own BSs and UL resources for transmission. The transmission power is controlled by themselves according to its locations. For a typical transmission, the other transmissions are assumed as interference. In another approach for the UL model in [3], cells are divided with respect to BSs. The set of active users which satisfy the cutoff threshold for the UL is able to communicate with their BSs. The cutoff threshold for the UL is the average received power required at the serving BS. For a typical active user operating on an allocated channel in its serving BS, the other active users on the channel in the other BSs are assumed to be as interferences. The model provides tractability by assuming that the interfering users constitute a PPP. Since the correlations among users occur by the locations of the associated BSs and the tagged channel, the assumption is required to provide the insights for the cellular UL performance. The performance of the UL with a resource management scheme also has been analyzed with the PPP as in the DL [13].

For the clustered network scenario, [15] and [16] is researched. In these works, clusters are formed based on parent PPP points. To model the clustered networks Mattĕrn cluster process (MCP) and Thomas cluster process (TCP) is used. The interference from the inter and the intra clusters are separately analyzed and approximated using the clustered process properties. The groups or clusters are already formed as a point process without the DL/UL joint model. And the process of forming clusters is not considered when leaders and members are independently deployed.

In addition, the stochastic geometry modeling has been developed by focusing on MAC schemes, especially Aloha-based schemes [17–19]. Since a node in an ad hoc network may operate as a transmitter or a receiver, an analytical model using PPP can be classified by the model of a receiver [6]. If each transmitter node has its corresponding receiver, the model is called as "Poisson bipolar model" [20–23]. In the Poisson bipolar model, the transmitters are modeled as a PPP and are divided into two non-overlapping subsets, whether a transmitter does its role at a specific time or not by using a TP. If the transmitter and receiver are independently modeled as PPPs, the model is called as "independent receiver model." In the model, a transmitter is controlled by TP and the transmission of the transmitter can be received by all subsets of the receivers [6]. When the transmitter is modeled as a PPP and the receiver is modeled as the subset of transmitters by using a specific condition, the model is called as "mobile ad hoc network model." If the set of active transmitters is classified by TP, the set of inactive transmitters at a slot is the set of receivers [24]. Note that a source node has to send data to its far destination node in a mobile ad hoc network. Then, the intermediate nodes are required to relay data to its destination node. If some of the inactive transmitters are in the direction from a source node to a destination node, they can be the receivers of the transmitter, i.e., the source node. In [22], the optimal TPs are derived for the maximum throughput medium access, the max-min fairness medium access, and the proportional fairness medium access. In [21], the performance of the Aloha protocol which is optimized for the proportional fair medium access is analyzed. The authors in [24] propose a spatial reuse Aloha protocol for a multihop network with the optimal TP which maximizes the density of progress, the mean total distance traversed in one hop by all transmissions initialized in some unit area. However, the optimal TP for the group communications with the DL coverage and the UL transmission has not been studied.

## 3 Slotted-Aloha-based access control schemes in group communication networks

In this section, we introduce the proposed SA-AC scheme which utilizes the optimal TP maximizing the DL/UL joint probability for the target distance. The target distance can be varied by the policy of the proposed SA-AC scheme. If the policy of the proposed SA-AC scheme is to maximize the coverage, the optimal TP is determined for maximizing the performance of the outermost members. In the example, the interference for the outermost members should be decreased to satisfy the UL threshold. The distance between the leader and the outermost member is affected by the DL threshold and the interference from the other leaders. Furthermore, since the number of members in the coverage of the leader increases by extending the coverage, the interference should be controlled by TP. So the proposed SA-AC scheme computes the optimal TP which is determined by considering the DL threshold, the UL threshold, the density of the leaders, the density of the members, and the target distance.

We present a network model for group communications and SA-AC schemes with various TP. The notations are summarized in Table 1. Both the group leaders and the group members are positioned according to PPPs. The leaders are distributed according to a PPP $\Phi_l$ with $\lambda_l$, the intensity of the leaders per unit area. The members are arranged according to a PPP $\Phi_m$ with $\lambda_m$, the intensity of the members per unit area. In the network model, let us define a link from a leader to a member as DL and a link from a member to a leader as UL. In the DL, we assume that a typical member is located at the origin. The typical member in the DL is denoted as $m$, and it is associated with the nearest leader among the leaders. The leader at the origin in the UL is denoted as $l$. Since the distributions are invariant, the locations of the leaders for the typical member in the UL are the same as those in the DL. Let $l_i$ denote the leader $i$ and $m_i$ be the member $i$ where $l_i \in \Phi_l \backslash l$ and $m_i \in \Phi_m \setminus m$.

We assume an interference-limited network in which the signal-to-interference ratios (SIRs) both in the DL and the UL are considered. The transmission powers of leaders and members are $P_l$ and $P_m$, respectively. The signals in both links experience the path loss. The path loss exponent is denoted as $\alpha$. The Rayleigh fading with the unit average power is assumed between any points. Let $h_{x,y}$ be the random variable to represent the channel effect from $x$ to $y$. Thus, the SIR at the receiver with the distance $r$ in the DL from $l$ to $m$ (SIR at a typical member in the downlink) is given by

$$\mathrm{SIR}_d(r) = \frac{P_l h_{l,m} r^{-\alpha}}{I_l}, \tag{1}$$

**Table 1** Summary of notations

| Notation | Description |
|---|---|
| $l$ | Leader at the origin in the uplink |
| $l_i$ | Leader $i$ |
| $m$ | Typical member in the downlink |
| $m_i$ | Member $i$ |
| $m_c$ | Set of covered members |
| $\Phi_l$ | PPP of leaders |
| $\Phi_m$ | PPP of members |
| $\Phi_{m_c}$ | Set of locations of covered members |
| $h_{x,y}$ | Channel effect from $x$ to $y$ |
| $\lambda_l$ | Intensity of leaders |
| $\lambda_m$ | Intensity of members |
| $P_l$ | Transmission power of leaders |
| $P_m$ | Transmission power of members |
| $\alpha$ | Pathloss exponent |
| $p_{d,u}$ | Downlink, uplink joint probability |
| $p_u$ | Uplink coverage probability |
| $p_d$ | Downlink coverage probability |
| $T_d$ | Downlink threshold |
| $T_u$ | Uplink threshold |
| $p_a$ | Access control probability |
| $r$ | Distance between $m$ and its nearest leader |
| $r_{d,i}$ | Distance between a leader $i$ and a typical member |
| $r_{u,i}$ | Distance between a member $i$ and a typical leader |
| $r_{du,i}$ | Distance between a covered member $i$ and a typical leader |
| $r_{tar}$ | Target distance |
| $\bar{r}_{max}$ | Average maximum distance between $l$ and its $m_c$ |
| $I_l$ | Cumulative interference from the leaders |
| $I_m$ | Cumulative interference from the members |
| $I_{m_c}$ | Cumulative interference from the covered members |
| $\tau$ | Transmission probability (TP) |
| $\tau^{dyn}$ | TP of the dynamic framed SA-AC |
| $\tau^{fix}$ | TP of the fixed framed SA-AC |
| $K$ | Frame size |
| $K^{dyn}$ | Frame size of the dynamic framed SA-AC |
| $K^{fix}$ | Frame size of the fixed framed SA-AC |
| $SIR_d$ | SIR at a typical member in the downlink |
| $SIR_u$ | SIR at a typical leader in the uplink |
| $SIR_{d,u}$ | SIR at a typical leader in the joint DL/UL transmission |
| $\bar{N}_m$ | Average number of the covered members per leader |
| $E_{ar}$ | Average achievable rate of covered members |

where $I_l$ is the cumulative interference from the leaders except the serving leader,

$$I_l = \sum_{l_i \in \Phi_l \backslash l} P_l h_{l_i,m} {r_{d,i}}^{-\alpha}, \tag{2}$$

where $r_{d,i}$ is the distance between a leader $i$ and a typical member. Since $r$ is invariant in the DL and the UL, the SIR at a typical leader in the UL is

$$\mathrm{SIR}_u(r) = \frac{P_m h_{m,l} r^{-\alpha}}{I_m}, \tag{3}$$

where $I_m$ is the cumulative interference from the members except the member $m$. In the UL, $I_m$ is given by

$$I_m = \sum_{m_i \in \Phi_m \backslash m} P_m h_{m_i,l} {r_{u,i}}^{-\alpha}, \tag{4}$$

where $r_{u,i}$ is the distance between a member $i$ and a typical leader.

The SA-AC scheme is assumed to work in a group communication network where the time slots are synchronized. One viable solution may be equipping global positioning system (GPS) modules on the leaders and the members since the signals from the GPS satellites provide the rather accurate timing and location information. There may be also several methods which can provide the synchronization to the members without GPS modules. Once a network is grouped into several clusters, all nodes can be bounded by the parent-children relationship. All members can be synchronized to the leader by periodically exchanging synchronization and acknowledgment packets with their corresponding leaders using pair-wise synchronization method [25, 26]. The location information may be piggybacked at the synchronization and acknowledgment packet for simultaneous time synchronization and location information distribution. Depending on the velocity of the nodes, the period between the synchronization and the location information distribution can be adjusted accordingly.

The time is divided into multiple slots, and they are partitioned into control slots and data slots. The leaders and the members transmit their data with the SA-AC scheme. A leader broadcasts a control frame in a synchronized control slot. The control frame of a leader includes the information for the group of the leader, the address of the leader, and the TC value. We assume that the TC value is shared by using a specific channel and they are identical among leaders. The control frame is decodable for a member when the SIR value is greater than the DL threshold, $T_d$. The member in the coverage of the leader is denoted as the covered member. Only the covered member joins the group of the nearest leader when the SIR value for the received control frame from the nearest leader is greater than $T_d$. Once the covered member decodes the control frame successfully, it gets the information to transmit its data frame to the leader in the UL. In the UL, the covered member transmits data frame in a data slot by using a TP. The TP is determined by the TC value and the type of the TC value depends on the type of the AC scheme. If the

SA-AC scheme uses the access control probability, $p_a$, as the TC value, the TP is given by

$$\tau = p_a. \tag{5}$$

In the SA-AC scheme using $p_a$, the covered members access each slot with $p_a$. If the SA-AC scheme uses the frame size as the TC value, the TP is given by

$$\tau = \frac{1}{K}, \tag{6}$$

where $K$ is the frame size which represents the number of data slots. In the SA-AC scheme using $K$, a covered member selects and accesses a slot among the $K$ slots. In general, $1/K$ is modeled as the access probability of the contenders in a slot. The framed SA-AC scheme consists of the fixed framed SA-AC scheme and the dynamic framed SA-AC scheme. The fixed framed SA-AC scheme utilizes the fixed TP which is determined by the fixed frame size [27]. Let $\tau^{fix}$ and $K^{fix}$ denote the TP and the frame size of the fixed framed SA-AC, respectively. The fixed framed SA-AC scheme utilizes $\tau^{fix} = 1/K^{fix}$. The dynamic framed SA-AC scheme utilizes the dynamic TP determined by the frame size which is dynamically changed according to the average number of the covered members per leader. The frame size in the dynamic framed SA-AC scheme is known to be optimal when the frame size is equal to the number of contenders [18, 28]. Let $\tau^{dyn}$ and $K^{dyn}$ denote the TP and the frame size of the dynamic framed SA-AC scheme, respectively. Then the dynamic framed SA-AC scheme utilizes $\tau^{dyn} = 1/K^{dyn}$.

However, if the channel effect and pathloss are not considered, such dynamic TP may not be optimal. So we need to find a new optimal TP maximizing the performance of group communications network. The optimal TP is affected by $\lambda_l$, $\lambda_m$, $T_d$, and $T_u$, where $T_u$ is the UL threshold. In addition, it has to be determined by considering the performance of the covered members. The performance varies by the distance between a leader and the members. In Fig. 1, an example of group communications network is shown. Fig. 1a presents the DL transmissions and Fig. 1b shows the UL transmissions. In DL, the leaders broadcast the control frames to the members. $\lambda_l$ determines the distance between a member and its nearest leader, and $T_d$ decides whether the member becomes the covered member. For example, in each group, three members near the leader become the covered members. These members receive the leader's control frames without channel error. Let the member with target distance $r_{tar}$ denote the target member. The target member in group 2 receives interference signal from the leaders in groups 1 and 3, but this interference signal is tolerable for reception.

In UL, the transmission of a member occurs when the member is in the coverage of the leader and determines whether the covered member participates in the UL transmission by $\tau$ and $T_u$. The target member in group 2 transmits data to the leader. The leader in group 2 receives interference signal from the member in group 2 as well as the members in groups 1 and 3. To decode the UL transmission of the target member, the interference signals have to be controlled by the optimal TP $\tau^*$ which is determined by $\lambda_l$, $\lambda_m$, $T_d$, $T_u$, and $r_{tar}$.

## 4 Optimal transmission probability for group communications

In this section, we derive the dynamic TP and the optimal TP. To derive the dynamic TP, we need the DL coverage probability and the average number of the covered members per leader. For the optimal TP, we need to derive the UL coverage probability and the DL/UL joint probability for a target distance. The target distance is the distance between a leader and a target member for which the DL/UL joint probability is maximized. Finally, we develop an analytical model for the performance of the SA-AC schemes using the dynamic TP and the optimal TP. From the model, we derive an optimal TP of the SA-AC scheme.

In our network model, both the leaders and the members are assumed to be arranged according to PPPs. Therefore, the pdf of the distance $R$ between a member and its nearest leader [4] can be expressed as

$$f_R(r) = 2\pi r\lambda_l \exp\left(-\pi r^2\lambda_l\right), \tag{7}$$

where $r$ is the distance between a member and its nearest leader. The members are divided into the covered members and the non-covered members by $T_d$. The following lemma provides the probability that a member is in the coverage of the nearest leader.

**Lemma 1** *For the DL threshold $T_d$, the DL coverage probability that a member with the distance $r$ from its nearest leader is in the coverage of the leader is*

$$p_d\left(r, T_d\right) = e^{-\pi r^2\lambda_l\zeta_l(T_d)}, \tag{8}$$

*where $\zeta_l(T_d) = T_d^{2/\alpha}\int_{T_d^{-2/\alpha}}^{\infty}\frac{1}{1+(u_l)^{\alpha/2}}\mathrm{d}u_l$. Then, the DL coverage probability that a member is in the coverage of the leader is*

$$p_d(T_d) = \frac{1}{1+\zeta_l(T_d)}. \tag{9}$$

*Proof* See Appendix A.1. □

Lemma 1 shows that $p_d(r, T_d)$ decreases by increasing $r$, $T_d$, and $\lambda_l$. Since the received signal strength from the nearest leader decreases as $r$ increases, $p_d(r, T_d)$ decreases. For a certain $r$, the SIR value may not be higher than $T_d$ for large $T_d$. Since the increase of $\lambda_l$ causes the increase of interference for a certain $r$, $p_d(r, T_d)$ decreases.

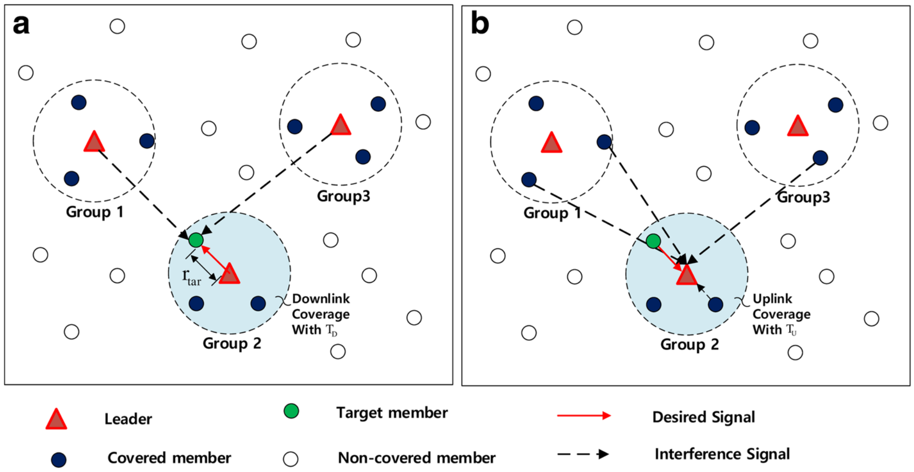


**Fig. 1** An example of group communications in a group communication network. **a** DL transmission. **b** UL transmission

Lemma 1 implies that the number of the covered members decreases by increasing $T_d$ for both $p_d(r, T_d)$ and $p_d(T_d)$. The expressions in Lemma 1 yield a closed-form when $\alpha = 4$, since $\zeta_l(T_d) = \sqrt{T_d}\left(\frac{\pi}{2} - \arctan\left(\frac{1}{\sqrt{T_d}}\right)\right)$.

From Lemma 1, we derive the dynamic TP, which determines the transmission probability of the covered members.

**Theorem 1** *For the DL threshold $T_d$, the dynamic TP that is dynamically changed by the number of the averaged covered members is*

$$\tau^{dyn} = \min\left(\frac{1}{\bar{N}_m}, 1\right) = \min\left(\frac{\lambda_l}{\lambda_m p_d\left(T_d\right)}, 1\right). \quad (10)$$

*Proof* If we assume that $S$ is the area of an entire network, $\bar{N}_m$ is obtained by dividing the average number of the covered members in $S$ by the average number of the leaders in $S$. Since the intensity of the covered members is $\lambda_m p_d(T_d)$, the average number of the covered members per leader $\bar{N}_m = \frac{\lambda_m p_d(T_d)S}{\lambda_l S} = \frac{\lambda_m p_d(T_d)}{\lambda_l}$ [5]. □

Theorem 1 shows that $\tau^{dyn}$ is adaptive to the number of the covered members per leader. We expect that $\tau^{dyn}$ decreases as $\bar{N}_m$ increases. It implies that the interference to the transmission of a typical covered member decreases as $\bar{N}_m$ increases. Since $\bar{N}_m$ is affected by $p_d(T_d)$, it increases by decreasing $T_d$. Thus, Theorem 1 indicates that $\tau^{dyn}$ decreases and the interference to the transmission of a typical covered member decreases as $T_d$ decreases in the dynamic framed SA-AC scheme.

Since the locations of the covered members are jointly changed by $T_d$ and the locations of the leaders, they are not PPP. It is challenging to model it accurately, but PPP approximation could be utilized [3]. In our model, we approximate them as a PPP. Let $\Phi_{m_c}$ and $\Phi_{m_o}$ denote the locations of the covered members and the locations of the non-covered members. We calculate the pdf of the distance between a leader and a covered member from the following theorem.

**Theorem 2** *The pdf of the distance between a leader and a covered member $m_c$ for a given $T_d$ is*

$$f_{R_{m_c}}(r) = \frac{2\pi r \lambda_l e^{-\pi r^2 \lambda_l (1+\zeta_l(T_d))}}{p_d(T_d)}. \quad (11)$$

*Proof* Since the coverage of a leader determines the distance between a leader and a covered member, the pdf is affected by the $T_d$. In our network model, the covered members are only able to transmit to their leader. Since the distribution of the distances between the leader and the members in DL is not changed in UL, the distribution of the distances between the leader and the covered members is induced by the pdf of $R$. In the UL transmission by using a TP, the interference from the covered members is obtained by normalizing the DL coverage probability at $r$ by $p_d(T_d)$. Thus, $f_{R_{m_c}}(r)$ is given by

$$f_{R_{m_c}}(r) = \frac{p_d(r, T_d) f_R(r)}{p_d(T_d)}. \quad (12)$$

Plugging $p_d(r, T_d)$ in (8) into (12), $f_{R_{m_c}}(r)$ is derived. □

Since $f_R(r)$ is conditioned by the DL coverage probability, $f_{R_{m_c}}(r)$ is affected by $T_d$. We expect that the increase of $T_d$ makes the pdf of $R_{m_c}$ within the DL coverage to increase. When $\alpha = 4$, both $p_d(r, T_d)$ and $p_d(T_d)$ have closed-form expressions, and $f_{R_{m_c}}(r)$ has also a closed-form expression. From Theorem 2, we derive the UL probability that the SIR value for the transmission of a covered member is larger than the UL threshold $T_u$. The SIR value in UL after DL is given by

$$\mathrm{SIR}_{d,u}(r) = \frac{P_m h_{m_c,l} r^{-\alpha}}{I_{m_c}}, \tag{13}$$

where $I_{m_c}$ and $SIR_{d,u}(r)$ are the cumulative interference from the covered members except for the $m_c$ at $l$ and the SIR value for the transmission of the $m_c$ at $l$ with the distance $r$ (SIR at a typical leader in the joint DL/UL transmission), respectively. In UL, $I_{m_c}$ is given by

$$I_{m_c} = \sum_{m_{c,i} \in \Phi_{m_c} \setminus m_c} P_m h_{m_{c,i},l} \left( r_{du,i}^{-\alpha} \right), \tag{14}$$

where $r_{du,i}$ is the distance between a covered member $i$ and a typical leader.

**Lemma 2** *For $\tau$, the UL coverage probability that the SIR value for the transmission of the covered member with the distance $r$ from its leader exceeds the UL threshold $T_u$ is*

$$p_u(r, \tau, T_u) = \exp\left(-\pi r^2 \lambda_m p_d(T_d) \zeta_m(T_u) \tau\right), \tag{15}$$

*where* $\zeta_m(T_u) = T_u^{2/\alpha} \frac{2\pi/\alpha}{\sin(2\pi/\alpha)}$.

*Proof* See Appendix A.2. □

Lemma 2 shows that $p_u(r, \tau, T_u)$ decreases by increasing $r$, $T_u$, and $\lambda_m$. Since the received signal strength from the covered member decreases as $r$ increases, $p_u(r, \tau, T_u)$ decreases. For a certain $r$, the SIR value for the signal may be hard to exceed $T_u$ for large $T_u$. Since the increase of $\lambda_m$ incurs the increase of the interference, $p_u(r, \tau, T_u)$ decreases. The expression in Lemma 2 is a closed-form when $\alpha = 4$, since $\zeta_m(T_u) = \frac{\pi}{2}\sqrt{T_u}$. The following lemma provides the DL/UL joint probability which quantifies the performance of the SA-AC scheme with $\tau$. We define the target member which is a member with target distance, $r_{tar}$. The DL/UL joint probability denotes the probability that a member with $r_{tar}$ from its nearest leader is in the coverage of the leader, i.e., the DL SIR exceeds the DL threshold $T_d$, and the nearest leader is in the coverage of the member transmitting the UL signal with $\tau$, i.e., the UL SIR exceeds the UL threshold $T_u$. The performance of the DL/UL joint probability for the target member shows the effect of $\tau$ for $r_{tar}$.

**Lemma 3** *For $\tau$, the DL/UL joint probability that the DL/UL SIR value for a member with $r_{tar}$ from its nearest leader exceeds $T_d$ and $T_u$ is*

$$\begin{aligned} p_{d,u}\left(r_{tar}, \tau, T_d, T_u\right) &= p_d\left(r_{tar}, T_d\right) \tau p_u\left(r_{tar}, \tau, T_u\right) \\ &= \tau e^{-\pi (r_{tar})^2 (\lambda_l \zeta_l(T_d) + \lambda_m p_d(T_d) \tau \zeta_m(T_u))}, \end{aligned} \tag{16}$$

*where* $0 \le \tau \le 1$.

*Proof* By letting $r = r_{tar}$ in (7) and (15), $p_{d,u}(r_{tar}, \tau, T_d, T_u)$ is derived. □

Since the DL/UL joint probability is affected by $T_d$, $T_u$, and $r_{tar}$, it decreases by increasing them. However, if the SA-AC scheme uses $\tau^{dyn}$ as $\tau$, $\tau^{dyn}$ increases as $T_d$ increases. Thus, the DL/UL joint probability for the SA-AC scheme is sensitive to $T_d$. If $\alpha = 4$, the closed-form expression of Theorem 3 is derived from the closed-from expressions in Lemma 1 and Lemma 2. From Lemma 3, we expect that $\tau$ varies according to $r_{tar}$. Since $p_{d,u}(r_{tar}, \tau, T_d, T_u)$ has the global extreme values for $\tau$, the optimal $\tau$ can be derived (see Appendix A.3). We now derive the optimal TP that maximizes $p_{d,u}(r_{tar}, \tau, T_d, T_u)$.

**Theorem 3** *For $T_d$ and $T_u$, the optimal TP that maximizes the DL/UL joint probability of a target member with $r_{tar}$ is*

$$\tau^* = \min\left( \frac{1}{\pi (r_{tar})^2 \lambda_m p_d(T_d) \zeta_m(T_u)}, 1 \right). \tag{17}$$

*where* $0 \le \tau^* \le 1$.

*Proof* The maximum DL/UL joint probability is found by

$$\frac{\partial p_{d,u}\left(r_{tar}, \tau, T_d, T_u\right)}{\partial \tau} = 0. \tag{18}$$

Thus the optimum $\tau$ is derived.

$$\tau^* = \frac{1}{\pi (r_{tar})^2 \lambda_m p_d(T_d) \zeta_m(T_u)}. \tag{19}$$

Since $\tau^* \le 1$ in a slot, $\tau^* = 1$ when $r_{tar} < \sqrt{1/\pi \lambda_m p_d(T_d) \zeta_m(T_u)}$. □

From Theorem 3, we derive $\tau^*$ to maximize the DL/UL joint probability for $\bar{r}_{max}$. $\bar{r}_{max}$ is the average maximum distance between a leader and its covered member. In general, since $r_{tar}$ has to be estimated by the target member and reported to the leader, $\bar{r}_{max}$ is hard to be known. However, if we assume that $\lambda_m$, $T_d$, and $T_u$ are given, $\tau^*$ can be obtained by the average number of the covered members as in the dynamic TP. The average number of the covered members can be known by using the number of associated members. Since the number of the covered members within the distance $r_{tar}$ is $\pi (r_{tar})^2 \lambda_m p_d(T_d)$, $\bar{N}_m = \pi (\bar{r}_{max})^2 \lambda_m p_d(T_d)$. So $\bar{r}_{max} = \sqrt{\frac{\bar{N}_m}{\pi \lambda_m p_d(T_d)}} = \sqrt{\frac{1}{\pi \lambda_l}}$ by plugging $\bar{N}_m$ in Theorem 1. Thus, $\tau^* = \min\left( \frac{1}{\bar{N}_m \zeta_m(T_u)}, 1 \right)$. It implies that $\tau^*$ for the average number of the covered members is the same as $\tau^*$ for $\bar{r}_{max}$ in the proposed SA-AC scheme.

We now derive the average achievable rate to measure the spectral efficiency performance of the SA-AC schemes. The average achievable rate for a target member with $r_{tar}$ and the average achievable rate of the members are obtained.

**Lemma 4** *For $T_d$ and $\tau$, the average achievable rate for a target member with $r_{tar}$ is*

$$E_{ar}(r_{tar}, \tau) = \tau \mathbb{E}_{\mathrm{SIR_{d,u}(r_{tar})}} \left[ ln \left[ 1 + SIR_{d,u}(r_{tar}) \right] | r_{tar} \right], \quad (20)$$

*where*

$$\mathbb{E}_{\mathrm{SIR_{d,u}(r_{tar})}} \left[ ln \left[ 1 + SIR_{d,u}\left(r_{tar}\right) \right] | r_{tar} \right] = \int_0^\infty \exp\left( -\pi \lambda_m p_d(T_d) \tau (r_{tar})^2 (e^t - 1)^{2/\alpha} \int_0^\infty \frac{1}{1 + \left(u_{ar,r_{tar}}\right)^{\alpha/2}} \mathrm{d}u_{ar,r_{tar}} \right) \mathrm{d}t. \quad (21)$$

*Furthermore, the average achievable rate of the covered members is*

$$E_{ar}(\tau) = \tau \int_0^\infty \frac{1}{1 + \frac{\pi}{2} \frac{\lambda_m p_d(T_d)^2 \tau}{\lambda_l} \left(e^t - 1\right)^{1/2}} \mathrm{d}t. \approx \frac{\lambda_l}{\lambda_m p_d(T_d)^2}. \quad (22)$$

*Proof* See Appendix A.4. □

Both metrics are computed by averaging the UL coverage probability when the transmission of a covered member is governed by $\tau$. The average achievable rate of a covered member is derived from the average achievable rate for a target member. Both metrics are not closed-form expressions, and the numerical integration is required to compute them.

## 5 Numerical results

In this section, we show the numerical results for the analytical models and simulation results with DL threshold $T_d$ and UL threshold $T_u$. We use the path-loss exponent $\alpha = 4$, the transmit power of a leader $P_l = 1$ W, and the transmit power of a member $P_m = 1$ W [20]. The transmission of both the leaders and the members in a single channel is done in multiple time slots. The leader intensity $\lambda_l = 3$ leaders/km$^2$ and the member intensity $\lambda_m = 20$ members/km$^2$ [29]. Both the leaders and the members are distributed with their intensity in a 25-km$^2$ area. And we focus on the sample area in a 1-km$^2$ area to evaluate the performance. Thus, the numerical results within the sample area are obtained in the simulation. In DL, each member computes the DL SIR and checks the DL SIR if it exceeds the DL threshold $T_d$. If the DL SIR exceeds the DL threshold $T_d$, the member becomes the covered member. In UL, the covered members transmit their signals according to the TP which is determined by the traditional SA-AC schemes and the proposed SA-AC scheme. The leader computes the UL SIR for each of the covered members and checks if the UL SIR exceeds the UL threshold $T_u$. if the UL SIR exceeds the UL threshold $T_u$, the DL/UL of the covered member is successful. We compare the performance of the SA-AC scheme with $\tau^*$ to those of the SA-AC schemes with $\tau^{dyn}$ as in Theorem 1 and $\tau^{fix}$ as in [27].

In Fig. 2, we verify the proposed SA-AC scheme by comparing the performance of the analysis and the simulation.

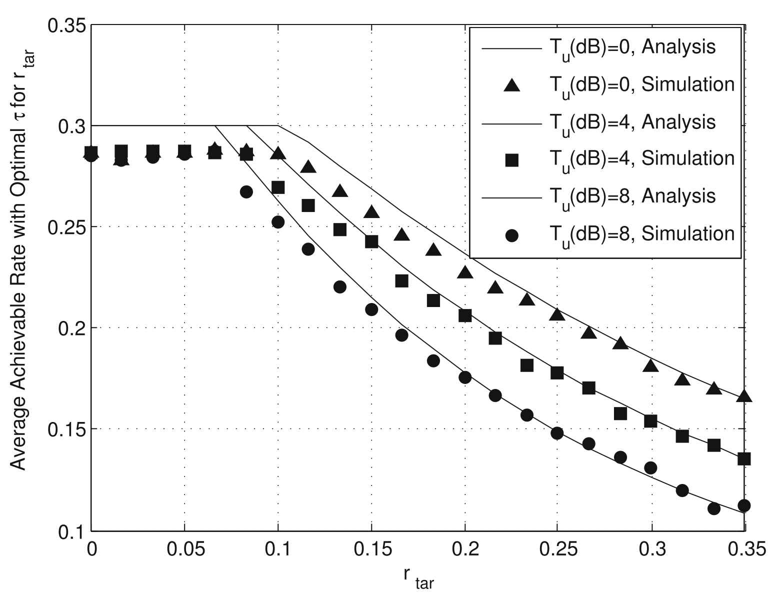


**Fig. 2** Average achievable rate with the optimal TP for varying target distance with different $T_u$ when $T_d$(dB)=−10 (marker: simulation, line: analysis)

The average achievable rate with the optimal $\tau$ is presented by varying $r_{tar}$. Since the performance is analyzed with the PPP assumption, $T_d$ is set to $-10$. The difference between the results is caused by the effect of approximation for the distribution of the covered members. The distribution of the covered members in the simulation is approximated by PPP in the analysis. The lower $T_d$ is selected, the closer the distribution of the covered members in the simulation approaches that of PPP. The exact distribution is not yet discovered [30]. The difference can be explained by the dependence between the covered members and their leaders. The dependence inherits from $T_d$. Since the locations of the covered members are jointly changed by $T_d$ and the locations of the leaders, they are not exact PPP. Since the SIR of the DL transmission is difficult to exceed $T_d$ as the distance between a covered member and its leader increases, the average maximum distance between a covered member and its leader decreases as $T_d$ increases. So the distance between the covered member and its leader is not independent. The dependence can be relaxed as $T_d$ decreases. Since the DL coverage probability increases as $T_d$ decreases, the area of a coverage area becomes larger and the distribution of the covered members approaches the PPP distribution of the members.

Since $r_{tar}$ is the distance between the target member and its leader, the signal strength of the target member decreases as $r_{tar}$ increases. Since $\tau$ is the TP of the covered members in a slot, the number of the covered members participating in the transmission in a slot increases as $\tau$ increases. The signals of the covered members except the target member become the interference to the target member. Thus, for the target member with $r_{tar}$, the SIR of the target member decreases as $r_{tar}$ increases or $\tau$ increases. Since the average achievable rate of a target member with $r_{tar}$ decreases as the SIR decreases, it also decreases as $r_{tar}$ increases or $\tau$ increases. If $r_{tar}$ decreases or $\tau$ decreases, the average achievable rate for a target member with $r_{tar}$ increases. Since the optimal $\tau$ decreases by $(r_{tar})^2$ as in Theorem 3, the interference decreases as $r_{tar}$ increases. However, the signals of the target member and its leader become weaker by $\alpha$ and the number of the transmissions decreases as the optimal $\tau$ decreases, then the average achievable rate of the covered member with the optimal $\tau$ decreases as $r_{tar}$ increases even if the interference decreases as the optimal $\tau$ decreases.

In Fig. 3, the performance of the DL/UL joint probabilities for varying $\tau$ is shown with different $r_{tar}$ when $T_d(dB) = -10$ and $T_u(dB) = 0$. The number of transmission members increases as $\tau$ increases. Since the interference increases as the number of transmission members increases, the SIR for the member with $r_{tar}$ decreases by increasing $\tau$. However, when the SIR for the member with $r_{tar}$ exceeds $T_u$ even if the interference for the member increases, $p_{d,u}(r_{tar}, \tau, T_d, T_u)$ increases as $\tau$ increases. Once the maximum $p_{d,u}(r_{tar}, \tau, T_d, T_u)$ is achieved, the performance starts to decrease by increasing $\tau$. The larger $r_{tar}$, the smaller value of the maximum $p_{d,u}(r_{tar}, \tau, T_d, T_u)$ is achieved. Since the signal becomes weaker as $r_{tar}$ increases, the SIR of the member with $r_{tar}$ is hard to exceed $T_u$ by increasing the number of the transmission members. Hence, $\tau$ has to be decreased to alleviate the interference and satisfy $T_u$ by reducing the number of the transmission members. Thus, $\tau$ to maximize $p_{d,u}(r_{tar}, \tau, T_d, T_u)$ decreases by increasing $r_{tar}$.

In Fig. 4, the performance of the optimal $\tau$ is shown for varying $r_{tar}$ with different $T_u$ when $T_d(dB) = -10$. When the signal strength of the member with $r_{tar}$ is enough to exceed $T_u$ even if all the covered members transmit their data frames, the optimal $\tau$ for $r_{tar}$ is one. The number of the inner members decreases and the signal strength increases as $r_{tar}$ decreases. So the optimal $\tau$ for $r_{tar}$ increases until one as $r_{tar}$ decreases. However, the optimal $\tau$ maximizing $p_{d,u}(r_{tar}, \tau, T_d, T_u)$ decreases by increasing $r_{tar}$ as shown in Fig. 3. The smaller $T_u$, the larger optimal $\tau$ is derived. Since the SIR for the member with $r_{tar}$ becomes easy to exceed $T_u$ as $T_u$ decreases, the optimal $\tau$ for $r_{tar}$ increases until the increase of the interference is tolerable to the member with $r_{tar}$.

In Fig. 5, the performance of the DL/UL joint probabilities is shown for varying $r_{tar}$ with the different SA-AC schemes when $T_d(dB) = -10$ and $T_u(dB) = 0$. We use the dynamic $\tau$ determined by (9) and (10), $\tau^{dyn} \approx 0.16$. Since the SIR of the member with $r_{tar}$ and the optimal $\tau$ to maximize $p_{d,u}(r_{tar}$ decreases as $r_{tar}$ increases, the performance of the SA-AC scheme with the optimal $\tau$ decreases as $r_{tar}$ increases. The performance of the SA-AC schemes with dynamic $\tau$ and fixed $\tau$ decreases as $r_{tar}$ increases. In the schemes with dynamic $\tau$ and fixed $\tau$, the values of $\tau$ do not vary for $r_{tar}$, and the SIR of the member with $r_{tar}$ may not exceed $T_u$ as $r_{tar}$ increases. When $r_{tar}$ is smaller than 0.1, the performance of the optimal $\tau$ is the same as the case with $K$ of 1. We can expect that the members within $r_{tar}$ satisfies $T_u$ even if all the members try to transmit data with $\tau = 1$. However, the DL/UL joint probability of the optimal $\tau$ is larger than that of the case with $K$ of 1 when $r_{tar} = 0.15$, since the members with $r_{tar}$ are strongly interfered by the inner members. The performance of the SA-AC scheme using the optimal $\tau$ approaches that of the SA-AC scheme using dynamic $\tau$ if $r_{tar}$ exceeds 0.1, since dynamic $\tau$ is almost the same as the optimal $\tau$ for $\bar{r}_{max}$. The optimal $\tau$ is adaptively determined by $r_{tar}$ while $\tau$ of the other schemes is not relevant to $r_{tar}$, thus $p_{d,u}(r_{tar}, \tau, T_d, T_u)$ is always maximized. Conversely, we can induce the distance whose DL/UL joint probability is maximized by $\tau$ of the other schemes.

In Fig. 6, the performance of the average achievable rate of the target member is shown for varying $r_{tar}$ with

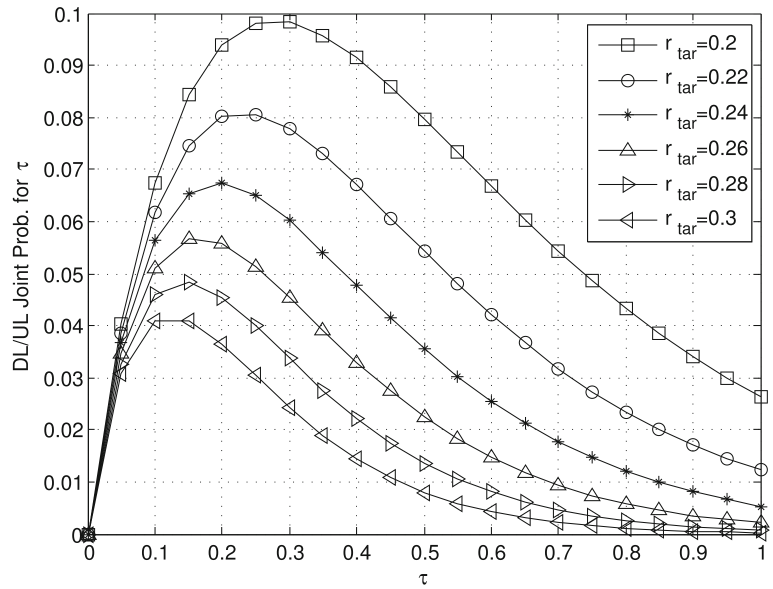


**Fig. 3** DL/UL joint probability for varying TP with different target distance when $T_d$(dB) $= -10$ and $T_u$(dB) $= 0$. It is shown that there are optimal TPs to maximize the DL/UL joint probability

the different SA-AC schemes when $T_d(dB) = -10$ and $T_u(dB) = 0$. We use the dynamic $\tau$ as in Fig. 5. Since the signal strength of the target member decreases and the optimal $\tau$ decreases to reduce the interference to the target member as $r_{tar}$ increases. So the SIR and the DL/UL joint probability for the member with $r_{tar}$ and the optimal $\tau$ decrease as $r_{tar}$ increases. In the SA-AC schemes with dynamic $\tau$ and fixed $\tau$, since the interference does not be alleviated by their TP, the performance of them decreases as $r_{tar}$ increases. However, the optimal $\tau$ case maintains the maximum performance. The optimal $\tau$ for $r_{tar}$ decreases so that the SIR for the target member with $r_{tar}$ satisfies $T_u$. However, since the case with $K$ of 1 case among the fixed $\tau$ is not adaptive to $r_{tar}$, the lowest performance is shown when $r_{tar}$ is larger than 0.2. The results show that the decrease of the DL/UL joint probability

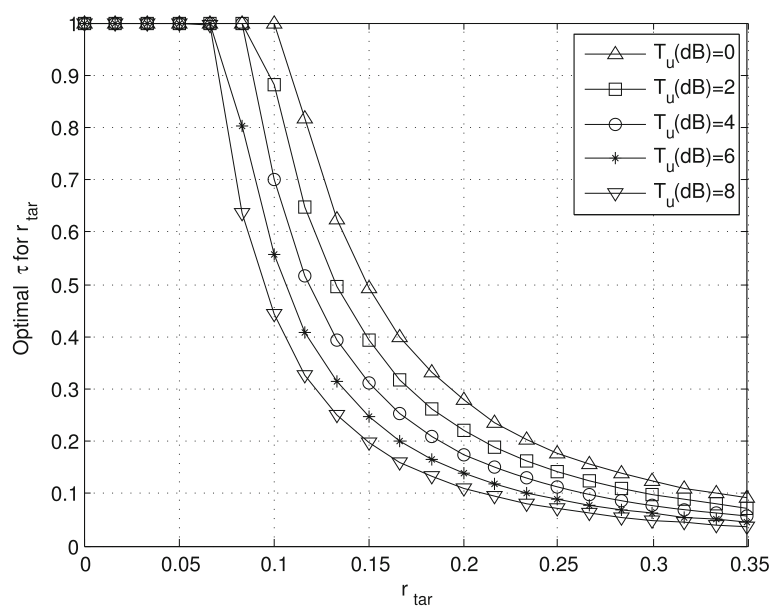


**Fig. 4** Optimal TP for varying target distance with different $T_u$ when $T_d$(dB)=-10. Since the influence of the interference is small in short target distance, the optimal TP is shown to be higher in shorter target distance

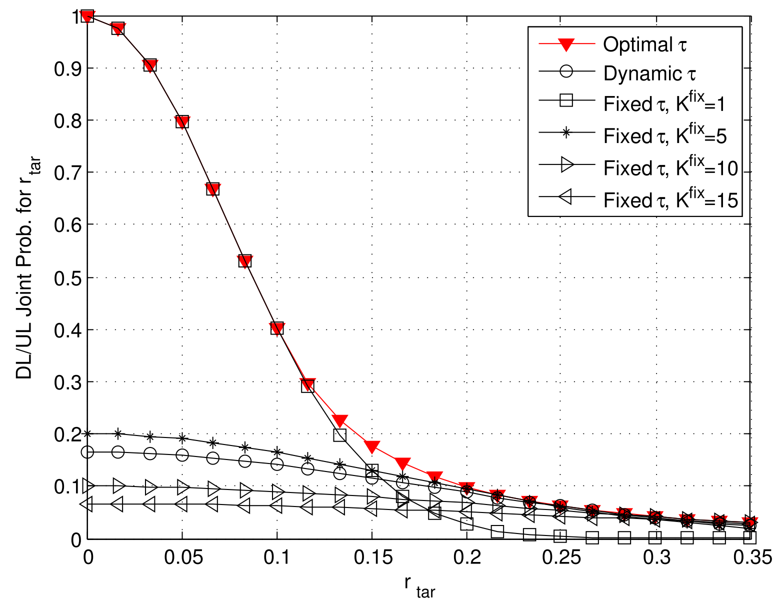


**Fig. 5** DL/UL joint probability for varying target distance with the different SA-AC schemes when $T_d(dB) = -10$ and $T_u(dB) = 0$. The proposed SA-AC scheme with optimal TP is shown to be the best by reflecting the spatial effect

induces the degradation of the average achievable rate for $r_{tar}$.

In Fig. 7, the performance of the DL/UL joint probability for the optimal $\tau$ and the performance of the UL probability to maximize the achievable rate UL$_{max}$ $\tau$ [20] are shown when $r_{tar} = 0.15$ is shown. Since the DL coverage probability decreases as $T_d$ increases, the number of the covered members decreases. Hence, the interference becomes weaker as $T_d$ decreases, and the SIR of the target member increases as $T_d$ increases. So the DL/UL joint probability increases as $T_d$ increases. Once $p_{d,u}(r_{tar}, \tau, T_d, T_u)$ is achieved, the performance starts to degrade by increasing $T_d$. For $r_{tar}$, the DL coverage probability of the target member decreases and the optimal

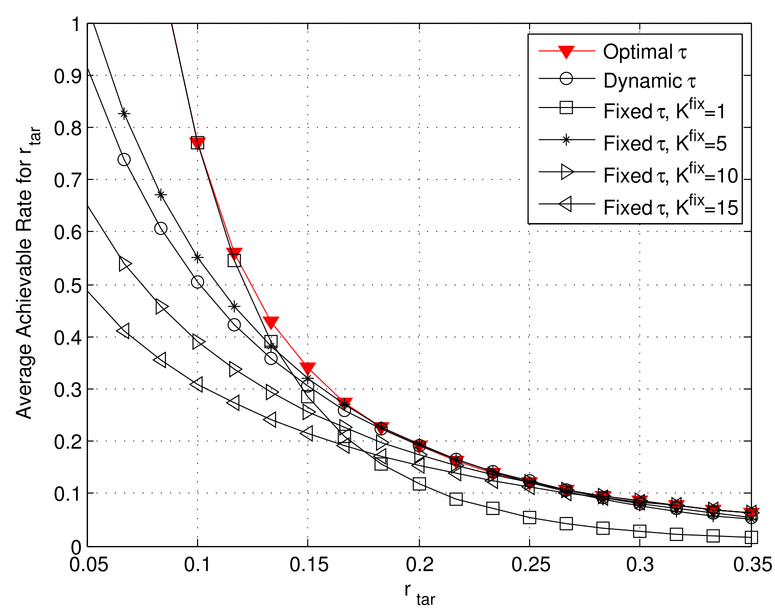


**Fig. 6** Average achievable rate for varying target distance with the different SA-AC schemes when $T_d(dB) = -10$ and $T_u(dB) = 0$. As in Fig. 5, the proposed SA-AC scheme with the optimal TP is shown to be the best

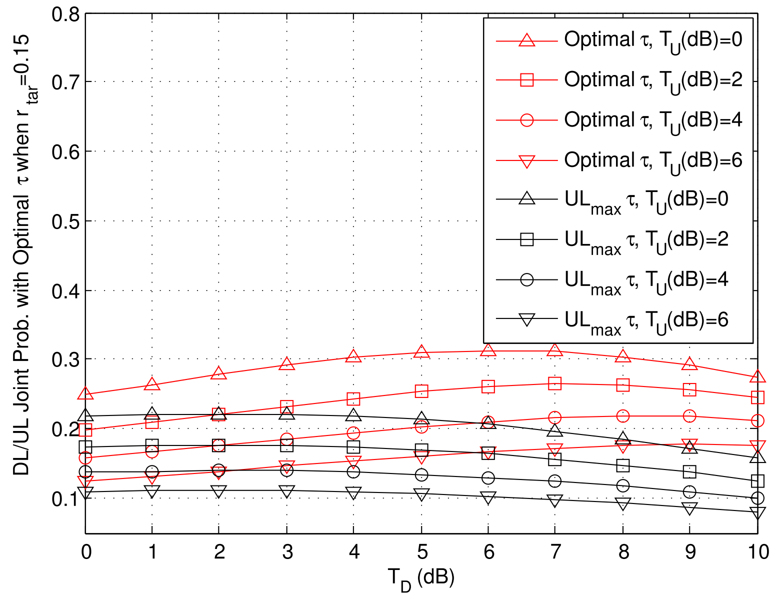


**Fig. 7** DL/UL joint probability with the optimal $\tau$ for varying $T_d$ with different $T_u$ when $r_{tar} = 0.15$

$\tau$ increases as $T_d$ increases. In addition, the DL coverage probability for a distance between a covered member and its leader increases as the distance decreases for $T_d$. Thus, the optimal $\tau$ of the covered member with smaller distance from the associated leader of the target member becomes larger. However, since the UL$_{max}$ $\tau$ is not designed to support group communications and does not consider the number of covered members by the DL threshold, i.e., UL$_{max}$ $\tau$ is determined to maximize the UL coverage probability only for the member intensity, the UL$_{max}$ $\tau$ is not changed as $T_d$ increases. So the number of transmissions of the covered members does not increase while the Interference decreases as the number of the covered members decreases. The UL SIR of the target member is hard to exceed $T_u$ after the maximum DL/UL joint probability. Since the UL coverage probability decreases as $T_u$ increases, the DL/UL joint probability decreases.

In Fig. 8, the performance of the average achievable rate with the optimal $\tau$ and the UL$_{max}$ $\tau$ for $\bar{r}_{max}$ is shown

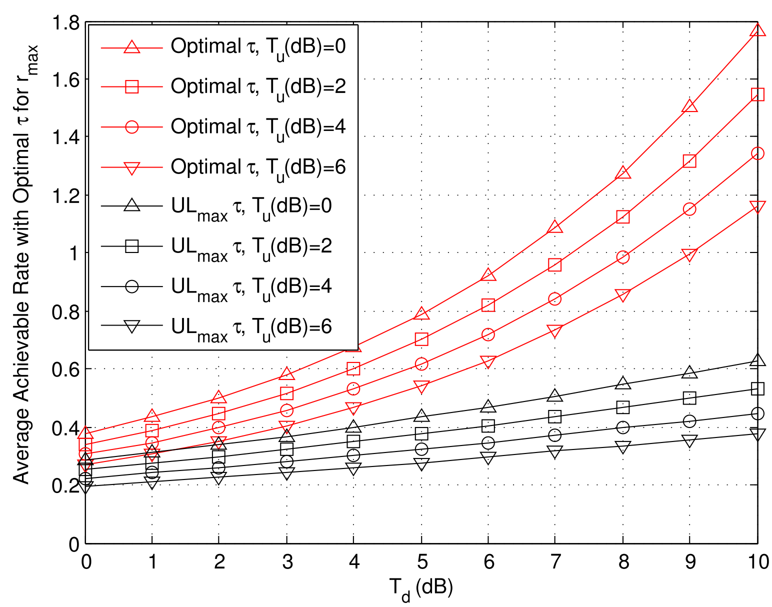


**Fig. 8** Average achievable rate with the optimal $\tau$ for varying $T_d$ with different $T_u$

for varying $T_d$ with different $T_u$. The optimal $\tau$ for $\bar{r}_{max}$ varies according to $T_d$ and $T_u$. Since the increase of $T_d$ reduces the number of the covered members, the interference for a covered member decreases as $T_d$ increases. And the signal strength of a covered member increases as the distance between the covered member and its leader decreases. Then the SIR of the member increases and it is sufficient to exceed $T_u$. Therefore, the performance of the average achievable rate increases by increasing $T_d$. The lower $T_u$, the larger the UL coverage probability becomes by increasing the optimal $\tau$. Thus, the average achievable rate with the optimal $\tau$ is maximized by increasing $T_d$ when $T_u(dB) = 0$. However, since the UL$_{max}$ $\tau$ is not changed for the coverage of the leader, it is not possible for the covered members to increase the numbers of transmissions. Although the SIR of the covered member increases by the increase of the signal strength and the decrease of the interference, the UL$_{max}$ $\tau$ might not be sufficient to increase the number of successful covered members in DL/UL.

## 6 Conclusions

In this paper, we have proposed an SA-AC scheme and developed an analytical model of the SA-AC schemes for group communications network. The proposed analytical model is affected by the intensity of leaders, the intensity of members, and the thresholds for DL and UL which are the important factors of service quality. The proposed analytical model presents the optimal TP to maximize the DL/UL joint probability at a target distance. Since the importance of the DL/UL joint probability at a target distance varies with the type of service, the optimal TP is carefully determined for providing services efficiently. The proposed analytical model has been validated via simulations, and the performance of the SA-AC schemes has been demonstrated. For group communications, the DL/UL joint probability at a target distance can be maximized by the proposed SA-AC scheme, which is superior to other schemes for the target distance. As a result, the importance of considering DL/UL joint probability in the group communication network has been proven.

## Appendix

### A.1 Proof of Lemma 1

For the DL threshold $T_d$, the DL coverage probability that a member with the distance $r$ from its nearest leader is

$$\begin{aligned} p_d(r, T_d) &= \mathbb{P}\left[\mathrm{SIR}_d(r) > T_d | r\right] \\ &= \mathbb{P}\left[h_{l,m} > P_l^{-1} r^{\alpha} I_l T_d | r\right] \\ &= \mathbb{E}\left[\exp\left(P_l^{-1} r^{\alpha} I_l T_d\right) | r\right] \\ &= \mathcal{L}_{I_l}\left(P_l^{-1} r^{\alpha} T_d\right), \end{aligned} \tag{23}$$

where $\mathcal{L}_{I_l}(s)$ is the Laplace transform of the aggregate interference received at the leader. $\mathcal{L}_{I_l}(s)$ can be expressed as

$$\begin{aligned} &\mathcal{L}_{I_l}(s) \\ &\quad= \mathbb{E}_{I_l}\left[e^{-sI_l}\right] \\ &\quad= \mathbb{E}_{\Phi_l, h_{l_i,m}}\left[e^{-s\left(\sum_{l_i \in \Phi_l \setminus l} P_l h_{l_i,m} r_{d,i}^{-\alpha}\right)}\right] \\ &\quad= \mathbb{E}_{\Phi_l}\left[\prod_{l_i \in \Phi_l \setminus l} \mathbb{E}_{h_{l_i,m}}\left[e^{-h_{l_i,m}\left(sP_l r_{d,i}^{-\alpha}\right)}\right]\right] \\ &\quad\overset{(a_1)}{=} e^{-2\pi\lambda_l \int_r^{\infty}\left(1-\mathbb{E}_{h_{l_i,m}}\left[e^{-h_{l_i,m}\left(sP_l v_l^{-\alpha}\right)}\right]\right) v_l \mathrm{d}v_l} \\ &\quad= e^{-2\pi\lambda_l \int_r^{\infty}\left(1-\frac{1}{1+sP_l v_l^{-\alpha}}\right) v_l \mathrm{d}v_l} \\ &\quad\overset{(a_2)}{=} e^{-2\pi\lambda_l \int_r^{\infty}\left(\frac{1}{1+\left(v_l/\left(r(T_d)^{1/\alpha}\right)\right)^{\alpha}}\right) v_l \mathrm{d}v_l} \\ &\quad\overset{(a_3)}{=} e^{-\pi r^2 \lambda_l T_d^{2/\alpha} \int_{T_d^{-2/\alpha}}^{\infty} \frac{1}{1+(u_l)^{\alpha/2}} \mathrm{d}u_l} \\ &\quad\overset{(a_4)}{=} e^{-\pi r^2 \lambda_l \zeta_l(T_d)}, \end{aligned} \tag{24}$$

where $(a_1)$ is derived from the probability generating functional (PGFL) of PPP [31], $(a_2)$ uses $s = P_l^{-1} r^{\alpha} T_d$, $(a_3)$ is derived by the change of the variable $u_l = \left(v_l/r(T_d)^{1/\alpha}\right)^2$, and $(a_4)$ utilizes the change of the variable $\zeta_l(T_d) = T_d^{2/\alpha} \int_{T_d^{-2/\alpha}}^{\infty} \frac{1}{1+(u_l)^{\alpha/2}} \mathrm{d}u_l$. Thus, plugging (24) into (23), we obtain (8). And combining (23) with (7), we obtain the DL coverage probability that a member is in the coverage of its nearest leader given by

$$p_d(T_d) = \int_0^{\infty} p_d\left(r, T_d\right) f_R(r) \mathrm{d}r. \tag{25}$$

Lemma 1 and its derivation corresponds to the interference limited network case as in [4].

### A.2 Proof of Lemma 2

For the UL threshold $T_u$ and $\tau$, the UL coverage probability that the SIR value for the transmission of the covered member with the distance $r$ from its leader exceeds $T_u$ is given by

$$\begin{aligned} p_u(r, \tau, T_u) &= \mathbb{P}\left[\mathrm{SIR}_{d,u}(r, \tau) > T_u | r\right] \\ &= \mathbb{P}\left[h_{m_c,l} > P_m^{-1} r^{\alpha} I_{m_c} T_u | r\right] \\ &= \mathbb{E}\left[\exp\left(P_m^{-1} r^{\alpha} I_{m_c} T_u\right) | r\right] \\ &= \mathcal{L}_{I_{m_c}}\left(P_m^{-1} r^{\alpha} T_u\right) \end{aligned} \tag{26}$$

where $\mathcal{L}_{I_{m_c}}(s)$ denotes the Laplace transform of the aggregate interference received at the leader. $\mathcal{L}_{I_{m_c}}(s)$ can be found in a similar way to (24). Thus,

$$
\begin{aligned}
&\mathcal{L}_{I_{m_c}}(s)\\
&= \mathbb{E}_{I_{m_c}}\left[e^{-sI_{m_c}}\right]\\
&= \mathbb{E}_{\Phi_{m_c},h_{m_{c,i},l}}\left[e^{-s\left(\sum_{m_{c,i}\in\Phi_{m_c}\setminus m_c} P_m h_{m_{c,i},l} r_{du,i}^{-\alpha}\right)}\right]\\
&= \mathbb{E}_{\Phi_{m_c}}\left[\prod_{m_{c,i}\in\Phi_{m_c}\setminus m_c} \mathbb{E}_{h_{m_{c,i},l}}\left[e^{-h_{m_{c,i},l}\left(sP_m r_{du,i}^{-\alpha}\right)}\right]\right]\\
&= \exp\Bigg( -2\pi\lambda_m p_d(T_d)\tau\\
&\int_0^\infty \left(1-\mathbb{E}_{h_{m_{c,i},l}}\left[e^{-h_{m_{c,i},l}(sP_m v_m^{-\alpha})}\right]\right) v_m \mathrm{d}v_m\Bigg)\\
&= e^{-2\pi\lambda_m p_d(T_d)\tau \int_0^\infty \left(1-\frac{1}{1+sP_m v_m^{-\alpha}}\right]\Big) v_m \mathrm{d}v_m}\\
&\overset{(a_5)}{=} e^{-2\pi\lambda_m p_d(T_d)\tau \int_0^\infty \left(\frac{1}{1+\left(v_m/(r(T_u)^{1/\alpha})\right)^{\alpha}}\right) v_m \mathrm{d}v_m}\\
&\overset{(a_6)}{=} e^{-\pi r^2 \lambda_m p_d(T_d)\tau T_u^{2/\alpha} \int_0^\infty \frac{1}{1+(u_m)^{\alpha/2}}\mathrm{d}u_m}\\
&\overset{(a_7)}{=} e^{-\pi r^2\lambda_m p_d(T_d)\tau\zeta_m(T_u)}.
\end{aligned}
\tag{27}
$$

where $(a_5)$ is found from $s = P_m^{-1} r^\alpha T_u$, $(a_6)$ comes from the change of variable $u_m = \left(v_m/r(T_u)^{1/\alpha}\right)^2$, and $(a_7)$ is derived from the change of variables

$$
\zeta_m(T_u) = T_u^{2/\alpha}\int_0^\infty \frac{1}{1+(u_m)^{\alpha/2}}\mathrm{d}u_m = T_u^{2/\alpha}\frac{2\pi/\alpha}{\sin(2\pi/\alpha)}. \tag{28}
$$

### A.3 Proof of Optimal $\tau$

Let $f(\tau)$ be $p_{d,u}(r_{tar},\tau,T_d,T_u)$. By the extreme value theorem, if $f(\tau)$ is continuous in the interval of $\tau \in [0,1]$, then at some point of the interval, $f(\tau)$ attains a global maximum and a global minimum [32–34]. Then the point of attainment is either 1) a point where $f'(\tau)$ does not exist, 2) a point where $f'(\tau)=0$, and 3) a point at one end of the interval [33]. $f(\tau)$ can be expressed as

$$
f(\tau) = \tau\exp(-a-b\tau), \tag{29}
$$

where $a = \pi r_{tar}^2\lambda_l\zeta_l(T_d)$ and $b = \pi r_{tar}^2\lambda_m P_l^c(T_d)\zeta_m(T_u)$, $a \geq 0$ and $b \geq 0$. Since $f(\tau)$ is differentiable in $\tau \in [0,1]$, $f(\tau)$ is continuous and $f'(\tau)$ exists for all $\tau \in [0,1]$.

$$
f'(\tau) = (1-b\tau)\exp(-a-b\tau). \tag{30}
$$

When $\tau = \frac{1}{b}$, $f'(\tau)=0$. We evaluate $f(\tau)$ at the points where $f'(\tau)=0$ and at the end points as the candidates for the extreme values. The function value at the point where $f'(\tau)=0$ is

$$
f\left(\frac{1}{b}\right) = \frac{1}{b}\exp(-a-1), \tag{31}
$$

The function values at the end points are

$$
f(0) = 0, \tag{32}
$$

$$
f(1) = \exp(-a-b). \tag{33}
$$

Since $f(\tau)\geq 0$, $f(0)=0$ is the global minimum of $f(\tau)$.

If $0 \leq b < 1$, $\frac{1}{b} > 1$ and $f\left(\frac{1}{b}\right)$ is not defined in the interval of $\tau \in [0,1]$. Thus, $f(1)$ is the global maximum when $0 \leq b < 1$. If $b \geq 1$, then $be^1 \leq e^b$. Thus, $f\left(\frac{1}{b}\right) \geq f(1)$ can be verfied as follows.

$$
\frac{1}{be^1} \geq \frac{1}{e^b}. \tag{34}
$$

Thus, $f\left(\frac{1}{b}\right)$ is the global maximum of $f(\tau)$ when $b \geq 1$. Therefore an optimal $\tau$ exists for $f(\tau)$ in the interval of $[0,1]$.

### A.4 Proof of Lemma 4

For $T_d$ and $\tau$, the average achievable rate for a target member with $r_{tar}$ is given by

$$
\begin{aligned}
&E_{ar}(r_{tar},\tau)\\
&= \tau\int_0^\infty \mathbb{P}\left[\ln\left(1+\frac{P_m h_{m_c,l} r_{tar}^{-\alpha}}{I_{m_c}} > t\right)\right]\mathrm{d}t\\
&= \tau\int_0^\infty \mathbb{P}\left[h_{m_c,l} > P_m^{-1} r_{tar}^{\alpha} I_{m_c}(e^t-1)\right]\mathrm{d}t\\
&= \tau\int_0^\infty \mathbb{E}\left[\exp\left(P_m^{-1} r_{tar}^{\alpha} I_{m_c}(e^t-1)\right)\right]\mathrm{d}t\\
&= \tau\int_0^\infty \mathcal{L}_{I_{m_c}}\left(P_m^{-1} r_{tar}^{\alpha}(e^t-1)\right)\mathrm{d}t.
\end{aligned}
\tag{35}
$$

Similar to Appendix A.1 and Appendix A.2, it follows,

$$
\begin{aligned}
&\mathcal{L}_{I_{m_c}}\left(P_m^{-1} r_{tar}^{\alpha}(e^t-1)\right)\\
&= e^{-2\pi\lambda_m p_d(T_d)\tau\int_0^\infty \left(1-\frac{1}{1+(r_{tar}/v_m)^{\alpha}(e^t-1)}\right]\Big) v_m\mathrm{d}v_m}\\
&= e^{-2\pi\lambda_m p_d(T_d)\tau\int_0^\infty \left(\frac{1}{1+\left(v_m/\left(r(e^t-1)^{1/\alpha}\right)\right)^{\alpha}}\right) v_m\mathrm{d}v_m}\\
&\overset{(a_8)}{=} \exp\Bigg( -\pi\lambda_m p_d(T_d)\tau(r_{tar})^2(e^t-1)^{2/\alpha}\\
&\int_0^\infty \frac{1}{1+(u_{ar,r_{tar}})^{\alpha/2}}\mathrm{d}u_{ar,r_{tar}}\Bigg).
\end{aligned}
\tag{36}
$$

where $(a_8)$ uses the change variable $u_{ar,r_{tar}} = \left(\frac{v_m}{r_{tar}(e^t-1)^{1/\alpha}}\right)^2$.

When $\alpha = 4$ and $r_{tar} = r$, the average achievable rate of a covered member is then given by

$$
\begin{aligned}
&E_{ar}(\tau) \\
&= \tau \int_0^\infty \int_0^\infty \mathcal{L}_{I_{mc}}\left(P_m^{-1} r^\alpha \left(e^t - 1\right)\right) f_{R_{mc}}(r) \mathrm{d}t \mathrm{d}r. \\
&\overset{(a_9)}{=} \frac{\pi \lambda_l \tau}{p_d(T_d)} \int_0^\infty \frac{2 p_d(T_d)}{2\pi\lambda_l + \pi^2 \lambda_m p_d(T_d)^2 \tau (e^t - 1)^{1/2}} \mathrm{d}t. \\
&= \tau \int_0^\infty \frac{1}{1 + \frac{\pi}{2}\frac{\lambda_m p_d(T_d)^2 \tau}{\lambda_l}(e^t - 1)^{1/2}} \mathrm{d}t. \\
&\overset{(a_{10})}{\approx} \tau \int_0^\infty \frac{1}{\frac{\pi}{2}\frac{\lambda_m p_d(T_d)^2 \tau}{\lambda_l}(e^t - 1)^{1/2}} \mathrm{d}t. \\
&\overset{(a_{11})}{=} \tau \int_0^\infty \frac{1}{u^2 + C^2} \mathrm{d}u = \tau \left[\frac{1}{C} \arctan\left(\frac{u}{C}\right)\right]_0^\infty \\
&= \tau \frac{\pi}{2C} = \frac{\lambda_l}{\lambda_m p_d(T_d)^2}
\end{aligned}
\tag{37}
$$

where $(a_9)$ utilizes the change of the variable $z = r^2$ and (9) then change the order of integrals. $(a_{10})$ comes from the approximation of $1/\left(1 + a\sqrt{e^t + 1}\right)$ to $1/\left(a\sqrt{e^t + 1}\right)$ where $a > 0$. Also, $(a_{11})$ stems from the change of variables as $C = \frac{\pi \lambda_m p_d(T_d)^2 \tau}{2\lambda_l}$ and $u = C\sqrt{e^t - 1}$.

**Acknowledgements**

This work was supported by the National Research Foundation of Korea (NRF) grant funded by the Korean government (MSIP) (2015R1A2A2A01004067), and Basic Science Research Program through the NRF funded by the Ministry of Education (NRF-2010-0020210).

**Authors' contributions**

ML's contribution is writing the paper and conducting performance analysis and simulations. YK's contribution is partly writing the paper and conducting simulations. T-JL's contribution is writing and revising the paper and guiding the direction and organization of the paper. All authors read and approved the final manuscript.

**Competing interests**

The authors declare that they have no competing interests.

## Publisher's Note

Springer Nature remains neutral with regard to jurisdictional claims in published maps and institutional affiliations.

Received: 3 November 2016 Accepted: 10 August 2017
Published online: 24 August 2017

**References**

1. YS Kim, HB Lee, JS Kim, HJ Baek, MS Ryu, KS Park, in *Proc. of IEEE Information Technology Applications in Biomedicine (ITAB)*. ECG, EOG detection from helmet based system, (Tokyo, 2007), pp. 191–193. http://ieeexplore.ieee.org/document/4407378/
2. A Giorgetti, M Lucchi, M Chiani, MZ Win, Throughput per pass for data aggregation from a wireless sensor network via a UAV. IEEE Trans. Aerosp. Electron. Syst. **47**(4), 2610–2626 (2011)
3. H ElSawy, E Hossain, On stochastic geometry modeling of cellular uplink transmission with truncated channel inversion power control. IEEE Trans. Wirel. Commun. **13**(8), 4454–4469 (2014)
4. JG Andrews, F Baccelli, RK Ganti, A tractable approach to coverage and rate in cellular networks. IEEE Trans. Commun. **59**(11), 3122–3134 (2011)
5. H Jo, YJ Sang, P Xia, JG Andrews, Heterogeneous cellular networks with flexible cell association: a comprehensive downlink SINR analysis. IEEE Trans. Wirel. Commun. **11**(10), 3484–3495 (2012)
6. F Baccelli, B Bàszczyszyn, *Stochastic geometry and wireless networks in foundations and trends in networking*. (INRIA & Ecole Normale Superieure, 45 rue d'Ulm, Paris, 2009). https://hal.inria.fr/inria-00403040/file/FnT2.pdf
7. M Haenggi, Outage, local throughput, and capacity of random wireless networks. IEEE Trans. Wirel. Commun. **8**(8), 4350–4359 (2009)
8. H ElSawy, E Hossain, M Haenggi, Stochastic geometry for modeling, analysis, and design of multi-tier and cognitive cellular wireless networks: a survey. IEEE Commun. Surv. Tutor. **15**(3), 996-1019 (2013). Third Quarter
9. PD Mankar, G Das, SS Pathak, Modeling and coverage analysis of BS-centric clustered users in a random wireless network. IEEE Wirel. Commun. Lett. **5**(2), 208–211 (2016)
10. H Zhuang, T Ohtsuki, A model based on Poisson point process for analyzing MIMO heterogeneous networks utilizing fractional frequency reuse. IEEE Trans. Wirel. Commun. **13**(12), 6839–6850 (2014)
11. S Singh, JG Andrews, Joint resource partitioning and offloading in heterogeneous cellular networks. IEEE Trans. Wirel. Commun. **13**(2), 888–901 (2014)
12. TD Novlan, HS Dhillon, JG Andrews, Analytical modeling of uplink cellular networks. IEEE Trans. Wirel. Commun. **12**(6), 2669–2679 (2013)
13. TD Novlan, JG Andrews, Analytical evaluation of uplink fractional frequency reuse. IEEE Trans. Commun. **61**(5), 2098–2108 (2013)
14. AH Sakr, E Hossain, Analysis of K-Tier uplink cellular networks with ambient RF energy harvesting. IEEE J. Sel. Areas Commun. **33**(10), 2226–2238 (2015)
15. M Afshang, HS Dhillon, PHJ Chong, in *Proc.of IEEE Global Communications Conference (GLOBECOM)*. Coverage and Area Spectral Efficiency of Clustered Device-to-Device Networks, (San Diego, 2015). http://ieeexplore.ieee.org/document/7417450/
16. K Han, K Huang, Wirelessly powered backscatter communication networks: modeling, coverage, and capacity. IEEE Trans. Wirel. Commun. **16**(4), 2548–2561 (2017)
17. N Abramson, in *Proc.of AFIPS*. The Aloha system-another alternative for computer communications, vol. 36, (1970), pp. 281-285
18. JF Kurose, KW Ross, *Computer networking: a top-down approach, 6th edition*. (Pearson, 2012). https://www.pearson.com/us/higher-education/product/Kurose-Computer-Networking-A-Top-Down-Approach-6th-Edition/9780132856201.html
19. RTB Ma, V Misra, D Rubenstein, An analysis of generalized slotted Aloha protocols. IEEE/ACM Trans. Networking. **17**(3), 936–949 (2009)
20. F Baccelli, B Bàszczyszyn, P Mühlethaler, Stochastic analysis of spatial and opportunistic Aloha. IEEE J. Sel. Areas Commun. **27**(7), 1105–1119 (2009)
21. F Baccelli, B Błaszczyszyn, C Singh, in *Proc. of IEEE International Conference on Computer Communications (INFOCOM)*. Analysis of a proportionally fair and locally adaptive spatial Aloha in Poisson networks, (Toronto, 2014), pp. 2544–2552. http://ieeexplore.ieee.org/document/6848201/
22. F Baccelli, C Singh, in *Proc. of IEEE International Symposium and Workshops on Modeling and Optimization in Mobile, Ad Hoc and Wireless Networks (WiOpt)*. Adaptive Spatial Aloha, Fairness and Stochastic Geometry, (Tsukuba Science City, 2013), pp. 7–14. http://ieeexplore.ieee.org/document/6576400/
23. K Huang, V Lau, Y Chen, Spectrum sharing between cellular and mobile ad hoc networks: Transmission-Capacity Tradeoff. IEEE J. Sel. Areas Commun. **27**(7), 1256–1266 (2009)
24. F Baccelli, B Bàszczyszyn, P Mühlethaler, An Aloha protocol for multihop mobile wireless networks. IEEE Trans. Inf. Theory. **52**(2), 421–436 (2006)
25. Q Li, D Rus, Global clock synchronization in sensor networks. IEEE Trans.Comput. **55**(2), 214–226 (2006)
26. AB Kulakli, K erciyes, in *Proc. of IEEE International Symposium on Computer and Information Sciences (ISCIS)*. Time synchronization algorithms based on time-sync protocol in wireless sensor networks, (Istanbul, 2008), pp. 1–5. http://ieeexplore.ieee.org/document/4717888/
27. JE Wieselthier, A Ephremides, LA Michels, An exact analysis and performance evaluation of framed ALOHA with capture. IEEE Trans. Commun. **37**(2), 125–137 (1989)
28. FC Schoute, Dynamic frame length Aloha. IEEE Trans. Commun. COM-31. **31**(4), 565–568 (1983). http://ieeexplore.ieee.org/document/1095854/
29. SM Yu, S-L Kim, in *Proc. of IEEE International Symposium on Modeling & Optimization in Mobile, Ad Hoc & Wireless Networks (WiOpt)*. Downlink Capacity and Base Station Density in Cellular Networks, (Tsukuba Science City, 2013). http://ieeexplore.ieee.org/document/6576422/

30. YJ Sang, KS Kim, Load distribution in heterogeneous cellular networks. IEEE Commun. Lett. **18**(2), 237–240 (2014)
31. D Stoyan, W Kendall, J Mecke, *Stochastic geometry and its applications, 2nd edition*. (Wiley, 1996). https://www.amazon.com/Stochastic-Geometry-Its-Applications-2nd/dp/0471950998
32. EKP Chong, SH Zak, *An introduction to optimization, 2nd edition*. (Wiley, 2001). http://as.wiley.com/WileyCDA/WileyTitle/productCd-0471654000.html
33. AE Taylor, *Advanced calculus*. (Ginn, Boston, 1955). https://www.abebooks.co.uk/servlet/BookDetailsPL?bi=22425525610&searchurl=tn%3Dadvanced%2Bcalculus%26sortby%3D17%26an%3Dtaylor%2Ba%2Be
34. FD RL Finney, BK Demana, D Waits, *Kennedy, Calculus: graphical, numerical, algebraic*. (Prentice Hall, 2003). https://www.bookdepository.com/Calculus-Graphical-Numerical-Algebraic-Student-Edition-2003c-Ross-L-Finney/9780130631312